Third Gulf Conference on Roads (TGCR06), March 6-8, 2006 34-40

Numerical and Experimental Factorial Analysis of Pavements' Edge Failure

Mofreh F. Saleh*

Senior Lecturer, Department of Civil Engineering, University of Canterbury, Private Bag 4800, Christchurch, New Zealand

Abstract: Pavement edge failure has been encountered on many New Zealand state highways due to the lack of lateral support and the encroachment of heavy axle loads onto the edge of pavement. The main objective of this research work is to investigate the different factors affecting this type of distress. A three-dimensional finite elements model was designed to simulate different loading and shoulder conditions. A half fractional factorial experimental design was made to study five factors, namely, shoulder width, shoulder stiffness, axle load, tire pressure and pavement thickness. Each factor was studied at two levels to simulate extremely low and high conditions. Before carrying out the experimental analysis, a careful examination of the finite elements model was made to ensure accurate predictions. The multilayer elastic solution was carried out using Circly and Everstress software. The results of the multilayer and finite elements analyses were compared to actual measurements of vertical strains using the Transit New Zealand accelerated test track facility (CAPTIF). None of the models provided a perfect match between the measured and predicted vertical strains. The multilayer linear elastic solution and the three dimensional finite elements solutions were reasonably close. The order of importance of the different factors relies on the type of response and the location of that response. The shoulder stiffness was the most important factor affecting the maximum deflection under the outer wheel followed by the axle load, pavement thickness then shoulder width. For the compressive strain at the top of the subgrade and the maximum deflection between dual, the order of importance of factors was different. The shoulder stiffness, width and thickness played a significant role in distributing the stresses and strains on the top of the subgrade thus controlling the edge failure.

Keywords: Edge failure; Tire pressure; Axle load; Finite elements; Experimental design.

1. Introduction

From practical observation, it is apparent that failure near the edges of the pavement is common in New Zealand rather than the classic failure mechanisms of rutting or roughness. This failure mode is associated with the mountainous topography that makes constructing wide pavements expensive. When these relatively narrow pavements are subjected to heavy vehicles, the edges tend to crumble due to lack of lateral support.

Ball and Patrick (2005) carried out an investigation of the edge failure on New Zealand state highways and local authority roads utilizing data extracted from the Road Asset Maintenance Management system (RAMM) database. The data covered approximately 3,000 km of state highway and 3,000 km of local sealed roads. Besides basic data such as location, surface type, length of inspection site, traffic and heavy traffic levels, etc., the following factors were particularly selected for statistical analysis: lane width, number of lanes, length of unpatched edge breaks, length of patched edge breaks, terrain type, and radius of curvature of both lanes. They found that the principal factors affecting the occurrence of edge breaks are lane width, seal age and total traffic per lane. Seal age in itself made a significant contribution to the amount of edge breaks occurring. They concluded that because of the strong dependence of the probability of edge break on lane width, a research to improve the strength of the pavement edge would have a significant potential to improve rural road performance. The hypothesis forming the basis of the research is whether by providing support to the sides of the pavement using trenches containing high-strength material, failure should be prevented. As the strength, width and depth requirements of the lateral support are not known, the first stage of the research is to model and measure the stresses and strains generated by heavy traffic outside the wheel track.

A Finite Elements (FE) analysis of pavement stresses and strains is conducted at the University of Canterbury using general-purpose finite elements software. The results of the modelling will be compared with the measured strains using the Transit NZ CAPTIF accelerated testing facility located in Christchurch and the outcome of this comparison will be published somewhere else. Only limited amount of vertical strains measurements were used to validate the three-dimensional finite elements model and the results of this validation are shown in this paper.

The Canterbury Accelerated Pavement Testing Indoor Facility (CAPTIF) is located in Christchurch, New Zealand. It consists of a 58 m long (on the centerline) circular track contained within a 1.5 m deep by 4.0 m wide concrete tank so that the moisture content of the pavement materials can be controlled and the boundary conditions are known. A center platform carries the machinery and electronics needed to drive the system. Mounted on this platform is a sliding frame that can move horizontally by 1 m. This radial movement enables the wheel paths to be varied laterally and can be used to have the two "vehicles" operating in independent wheel paths.

At the ends of this frame, two radial arms connect to the Simulated Loading and Vehicle Emulator (SLAVE) units. These arms are hinged in the vertical plane so that

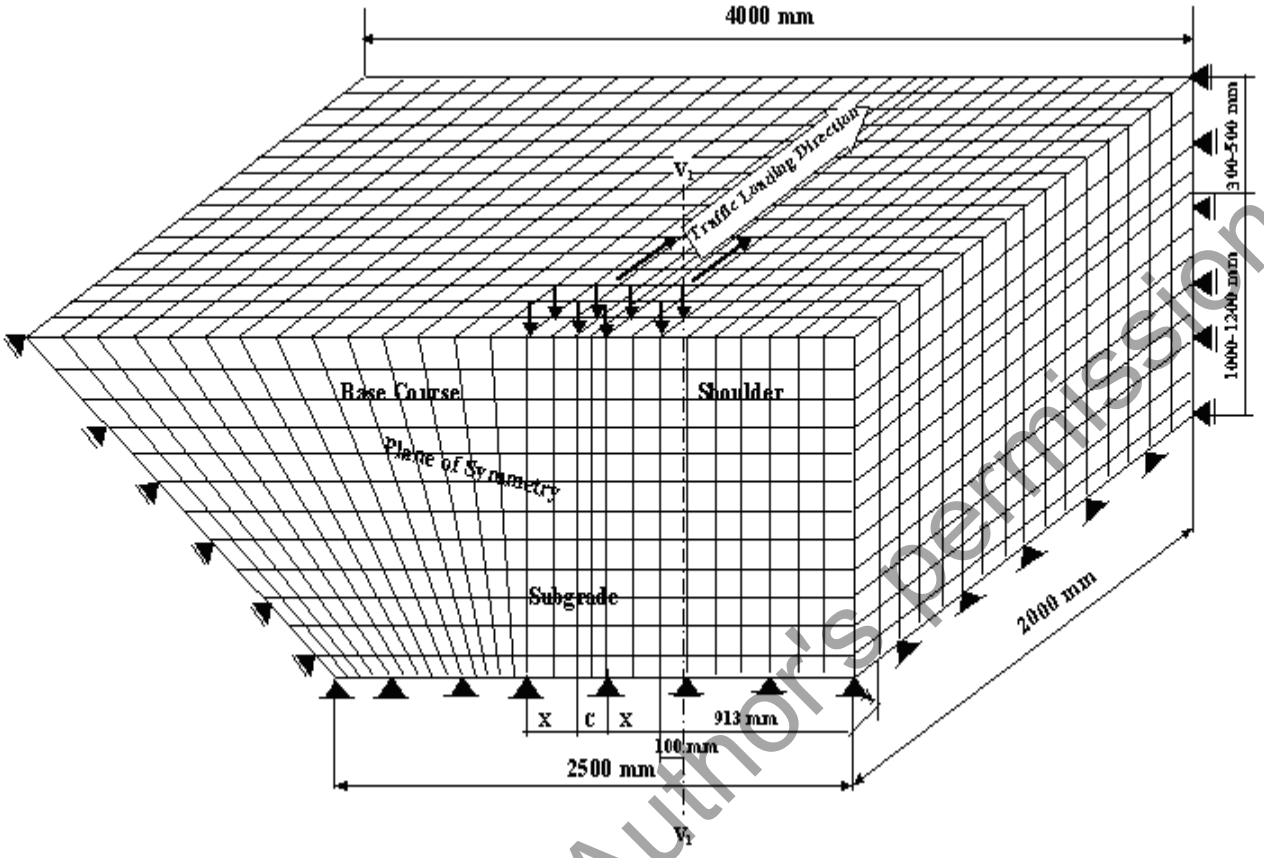

Figure 1. Three dimensional finite elements model

the SLAVE units can be removed from the track during pavement construction, profile measurement etc., and in the horizontal plane to allow normal vertical movement of the vehicles (Pidwerbesky, 1995).

2. Finite Elements Model

2.1 Model Geometry

ABAQUS (2003), a general-purpose finite elements code, was used to simulate the loading of a fully instrumented section in the accelerated test track, CAPTIF. The structural composition of this section is mainly made of chip sealed unbound base course over the subgrade as this type of construction is common in New Zealand. A half model was developed to reduce the computational effort by making use of the symmetry in the geometry and the loading. To carry out the experimental factorial design, different model geometries were considered. For example, two thicknesses for the base course were considered, 300 mm and 500 mm. The thickness of the subgrade is the difference between the CAPTIF tank depth (1500 mm) and the thickness of the base course. The 300 and 500 mm base course thicknesses were modelled using two and four elements, respectively. The thickness of the subgrade layer that ranges from 1000 to 1200 mm was modelled using eight and nine elements, respectively. The length of the finite elements section is 2000 mm. Figure 1 shows the three-dimensional finite elements model (3DFEM).

The loaded area is composed of eight elements, four elements in each half of the model. The loaded area is modelled based on tire imprints measurements carried out at the accelerated test track. It was found that the tire imprint width is 225 mm and the length of the tire imprint is 125 mm. However, these dimensions will vary based on the applied axle load and tire inflation pressure. In this analysis, the tire imprint width was maintained at 225 mm and the length of the tire imprint was calculated according to the applied load and tire pressure as shown below in Equation 1.

$$A = \frac{P}{q} \qquad (1)$$

A = Loaded area, m2
P= Total load per tire, kN
q = Tire Pressure, kPa

For example, for an axle load of 80 kN and a tire inflation pressure of 400 kPa,

$$\text{the loaded area under each tire} = A = \frac{20}{400} = 0.05\ \text{m}^2$$

X = 225 mm from actual measurements of the tire imprints at CAPTIF
*A = 2 * X * Y* (because this is half model), see Fig. 1.

Y = 111.1 mm

Where X is the width and Y is length of the loaded area

in each half of the 3DFEM. The clearance (C) between the two loaded areas is 125 mm.

The length of the loaded area varies for different axle loads and tire pressures and it can be calculated as shown above. For each run in the experimental factorial design, a separate 3DFEM model was developed to simulate the tire pressure, axle load, pavement thickness, and shoulder properties. The aspect ratio is defined as the ratio of maximum to minimum characteristic dimensions in the element. This ratio affects the distortion of the elements during analysis, and it should not exceed 4.0. In addition, a good practice is to choose corner angles in the range of 30° to 120° (Chandrupatla and Belegundu, 1996). The average aspect ratio for all models is 1.34 and the worst aspect ratio is 2.45. The average minimum and maximum corner angles are 75.95° and 104.06°, respectively.

2.2 Element Type

The finite elements model was built using continuum three dimensional, eight-node, reduced integration elements (C3D8R). The reduced integration elements are preferred over the fully integrated elements to avoid the shear locking, which is a problem with all fully integrated, first order, solid elements (ABAQUS, 2003). Shear locking only affects the performance of fully integrated elements that are subjected to bending loads.

2.3 Boundary Conditions

The rigid boundaries of the concrete tank in the accelerated test track, CAPTIF, were simulated in the finite elements model so that the bottom base of the subgrade is prevented from axial movements in the three directions. The sides of the model are only allowed to slide in the plane of the wall and are prevented from any movement perpendicular to the concrete wall. At the plane of symmetry, elements are only allowed to move vertically without any lateral displacement.

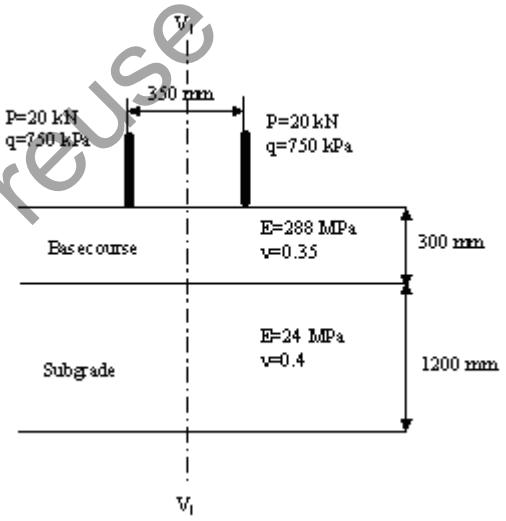

Figure 2. Multilayer elastic analysis model

2.4 Multilayer Elastic Analysis

The pavement structure was modelled as three layers subjected to dual load. The distance from center to center of the dual is 350 mm (350 mm = C+X = 125+225mm). Figure 2 shows the load configuration and pavement layers properties used in the verification analysis of the finite elements model.

3. Material Properties

The data from the repeated triaxial test for both the base course and the subgrade was used to determine the resilient modulus and the stress dependency of these materials. For the base course the k-θ model shown by Equation 2 and presented in Fig. 3 showed excellent fit for the triaxial data with a coefficient of determination (R^2) value of 99.3%.

$$M_r = 108.91 * \left(\frac{\theta}{P_{atom}} \right)^{0.723} \quad (2)$$

M_r = Resilient Modulus (MPa)
θ = Bulk stress (kPa)
P_{atom} = atmospheric pressure (P_{atom}=101.325 kPa)

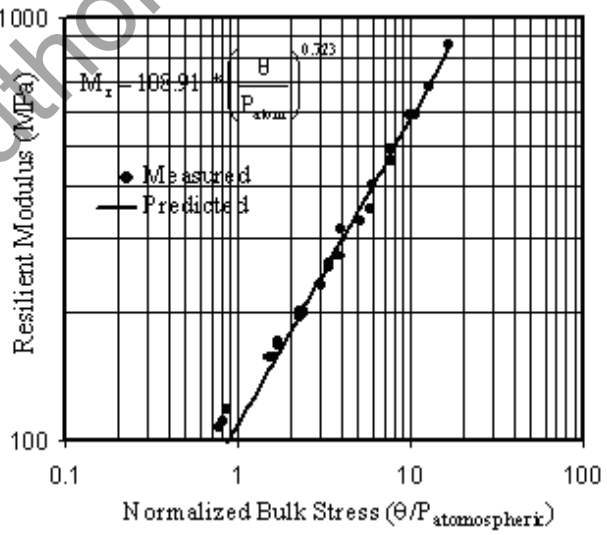

Figure 3. Relationship between resilient modulus and the bulk stress for the base course material

For linear elastic analysis, an average value of the resilient modulus of the base course and subgrade was calculated. The average resilient modulus for the base course is 288 MPa and that for subgrade is 24 MPa.

4. Verification of the 3DFEM

The pavement response predicted from the three dimensional finite elements (3DFEM) was compared with the multilayer elastic system solution. Linear and nonlinear elastic solutions were considered. In addition, isotropic and anisotropic analyses were carried out. The cross-anisotropic linear elastic solution was carried out using Circly software (Wardle, 1997). Evertress software (1999) was used to carry out the nonlinear and linear isotropic elastic solution. The solution shown here is for a tire pressure of 750 kPa and standard axle load of 80 kN and the material properties shown in Figs. 2 and 3. The verti-

cal compressive strains were determined at different depths under the centerline of the dual and compared with the measured strains in the accelerated test track facility (CAPTIF) as shown in Fig. 4

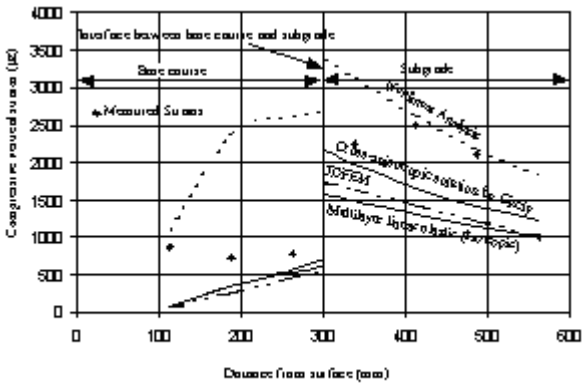

Figure 4. Comparisons between measured and predicted strains using different analytical methods

Figure 4 shows that none of the above mentioned methods perfectly matched the measured strained. The nonlinear analysis provided better match within the subgrade and showed significant deviation within the base course. The linear cross-anisotropic showed good match within the subgrade and similar match to the linear elastic isotropic solutions within the base course. The 3DFEM predictions were in the middle between the cross-anisotropic and the isotropic multilayer analysis. The predictions of the 3DFEM were considered acceptable and will suffice the purpose of this study.

5. Experimental Fractional Factorial Design

In the factorial experimental design, five factors; shoulder width, shoulder stiffness, axle load, tire pressure, and pavement thickness were examined. Table 1 shows the different factors and the level of each factor. Each factor was set at two extreme levels in order to span a wide range of each factor. For example, tire pressure was set at low value of 400 kPa and high value of 900 kPa while axle load spans a range from standard axle load (80 kN) to heavy axle load (120 kN). The shoulder stiffness varies from very weak material which is similar to the subgrade soil with resilient modulus 30 MPa to strong material which is similar to good quality base course with resilient modulus of 450 MPa. The width of the shoulder was measured from the outside edge of outer wheel load and ranges from 100 mm which represents extremely narrow shoulder with extreme encroachment from traffic, to 913 mm which is the maximum shoulder width in the Canterbury accelerated test track (CAPTIF) and that represents a relatively wide shoulder in rough terrain rural state highway. The thickness of the base course ranges from 300 mm to about 500 mm.

Table 1. The factors and levels studied in this simulation

Factors	Units	Levels	
		Low Level	High Level
Shoulder Width	mm	100	913
Shoulder Stiffness	MPa	30	450
Axle Load	kN	80	120
Tire Pressure	kPa	400	900
Pavement Thickness	mm	300	500

For full factorial experimental design, a five-factor experiment each at two levels requires $2^5 = 32$ runs. This is somehow large number of computations, therefore, a half fractional factorial design was utilized and this reduced the number of runs to 16 runs.

The pavement responses examined in this analysis are the maximum deflection between the dual, maximum surface deflection under the outer tire and the compressive stain at the top of the subgrade at a 300 mm distance from the center of the dual.

6. Results and Analysis of the Experimental Factorial Design

Table 2 shows the results of the 16 runs of the experimental design for three pavement responses, maximum deflection between dual (D_1), maximum deflection under the outer wheel (D_2), and the compressive strain on the top of the subgrade at a distance 300 mm from the center of the dual (300). In Table 2, a coded system was used to represent the low and high levels of each factor. In this system, code 1 is used to indicate the high level of the factor while -1 to indicate the low level of this factor. The actual values of each factor are shown in Table1.

Table 2. Experimental design results

Run	A	B	C	D	E	$\Delta_?$	Δ_2	ε_{300}
1	-1	-1	-1	-1	1	795	963	921
2	1	-1	-1	-1	-1	795	916	1169
3	-1	1	-1	-1	-1	802	912	1248
4	1	1	-1	-1	1	389	380	391
5	-1	-1	1	-1	-1	1231	1608	1962
6	1	-1	1	-1	1	697	963	1048
7	-1	1	1	-1	1	760	935	1273
8	1	1	1	-1	-1	1017	877	1026
9	-1	-1	-1	1	-1	869	1221	1337
10	1	-1	-1	1	1	869	1221	725
11	-1	1	-1	1	1	537	698	880
12	1	1	-1	1	-1	720	655	657
13	-1	-1	1	1	1	856	1317	1399
14	1	-1	1	1	-1	1214	1511	1753
15	-1	1	1	1	-1	1214	1511	1877
16	1	1	1	1	1	596	597	591

A = shoulder width (mm)
B = shoulder stiffness (MPa)
C = Axle load (kN)
D = Tire pressure (kPa)
E = Pavement thickness (mm) (the same as shoulder thickness)
D_1= Maximum deflection under the center of the dual (μ m)
D_2 = maximum deflection under the outer tire (μm)
ε_{300}= compressive strain on the top of the subgrade at 300 mm from the center of the dual (με).

The Design Expert software was used to carry out the analysis of the factorial design (Stat-Ease Inc.). Figure 5 shows the normal probability plot of effects for the maximum deflection between dual for the 16 runs. Effects which lie on the straight line are the insignificant effects, whereas the large effects are far from the line (Montgomery).

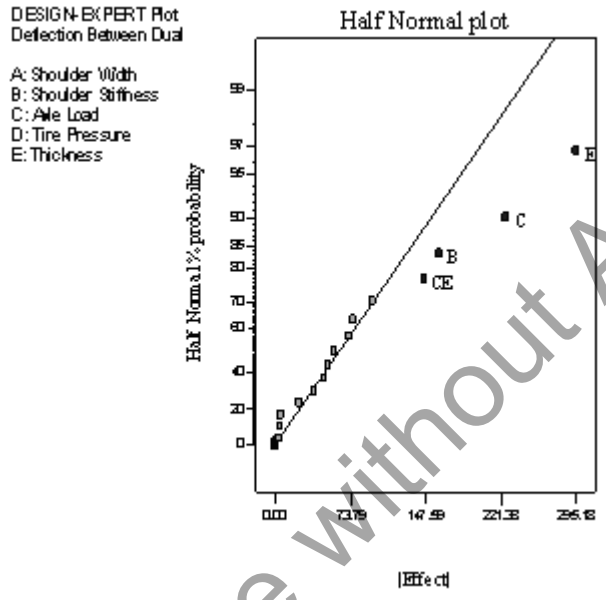

Figure 5. Significant factors affecting the maximum deflection between dual

Figure 5 shows that pavement thickness is the most significant factor affecting the maximum deflection between dual followed by the axle load, shoulder stiffness and the interaction between axle load and pavement thickness. Table 3 shows the analysis of variance (ANOVA) for the different factors. The model F-value of 16.55 implies the model is significant. There is only a 0.01% chance that a "Model F-Value" this large could occur due to noise. Values of "Prob > F" less than 0.0500 indicate model terms are significant. In this case B, C, E, CE are significant model terms.

Table 3. Analysis of variance (ANOVA) for selected factorial model for deflection between dual response

Source	Sum of Squares	DF	Mean Square	F Value	Prob>F
Model	$7.426*10^5$	4	$1.857*10^5$	16.55	0.0001
B	$1.040*10^5$	1	$1.040*10^5$	9.27	0.0112
C	$2.047*10^5$	1	$2.047*10^5$	18.25	0.0013
E	$3.485*10^5$	1	$3.485*10^5$	31.06	0.0002
CE	85455	1	85455	7.62	0.0186

Equation 3 represents the relationship between the predicted maximum deflection between the dual and the siginifcant parameters. The coefficient of determination of this model (R^2) is 85.8. Probabilty values greater than 0.1000 indicate the model terms are not significant. Figure 6 shows the normal probability plot of the residuals (the differences between the calculated and predicted values of deflection using Equation 3). When all the residual lie on a straight line on the probability chart, that means the model assumptions are correct (Montgomery).

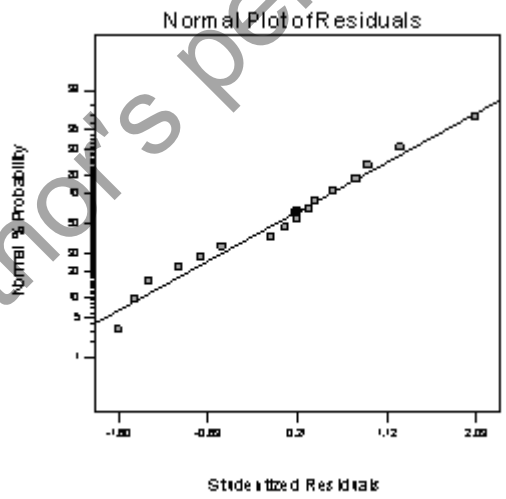

Figure 6. Normal probability plot of the residuals

$$\Delta_{Dual}(\mu m) = -509.66 - 0.384 * B + 20.27 * C + 2.178 * E - 0.0365 * C * E \qquad (R^2 = 85.8) \qquad (3)$$

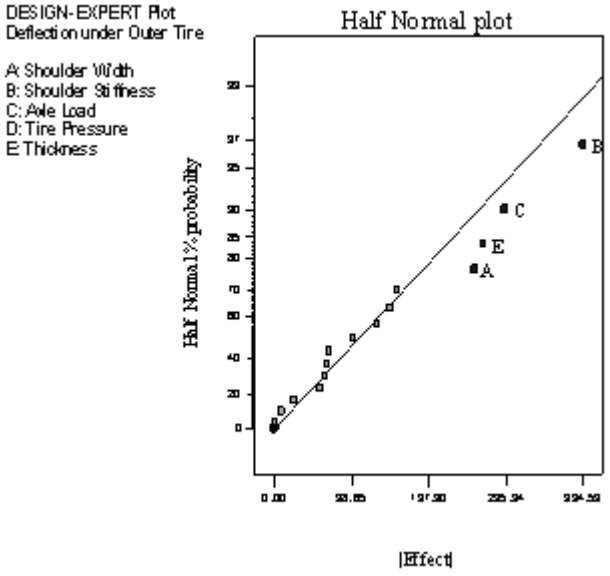

Figure 7. Significant factors affecting the maximum deflection under the outer tire

Figure 7 shows the order of importance of the factors affecting the maximum deflection under the outer wheel load. Shoulder stiffness played the most significant role followed by axle load, pavement thickness and shoulder width. Table 4 shows that the model F-value of 11.46 implies the model is significant. There is only a 0.06% chance that a "Model F-Value" this large could occur due to noise. Equation 4 represents the relationship between the maximum surface deflection under the outer wheel load as a function of the significant factors. The coefficient of determination is 80.6.

Table 4. Analysis of variance (ANOVA) for selected factorial model for the deflection under outer tire response

Source	Sum of Squares	DF	Mean Square	F Value	Prob > F
Model	$1.516E*10^6$	4	$3.790*10^5$	11.46	0.0006
A	$2.615*10^5$	1	$2.615*10^5$	7.91	0.0169
B	$6.228*10^5$	1	$6.228*10^5$	18.83	0.0012
C	$3.459*10^5$	1	$3.459*10^5$	10.46	0.0080
E	$2.858*10^5$	1	$2.858*10^5$	8.64	0.0135

$$\Delta_{Outer\ \ Tyre} = 1201.8 - 0.3145 * A - 0.9395 * B + 7.3522 * C \quad (R^2 = 80.6) \tag{4}$$

In studying the factors affecting the compressive strain on the top of the subgrade in the vicinity of the pavement shoulder (300 mm from the center of the dual), Fig. 8 shows that the most significant factor is the pavement thickness followed by axle load, shoulder width, shoulder stiffness and the interaction between shoulder width and stiffness. Table 5 shows that the Model F-value of 54.62 implies the model is significant. The relationship between the compressive strain at the top of the subgrade and the siginifcant factors is given by Equation 5. The coefficient of determination of this model is reasonably high (R^2=96.5).

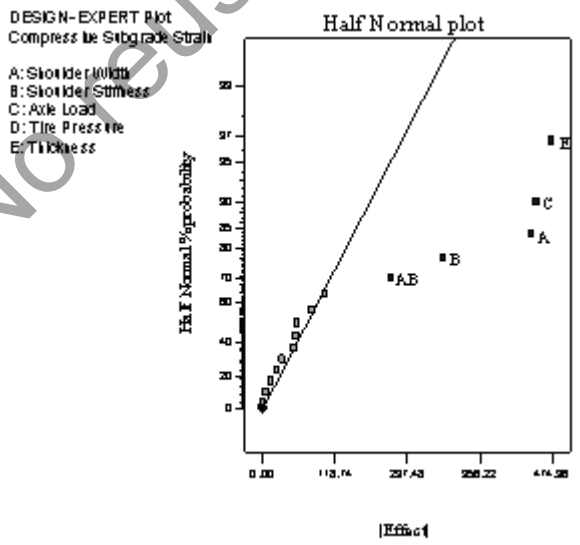

Figure 8. Significant factors affecting the compressive strain on the top of the subgrade

Table 5. Analysis of variance (ANOVA) for selected factorial model for compressive strain on the top of the subgrade

Source	Sum of Squares	DF	Mean Square	F Value	Prob> F
Model	$3.024*10^6$	5	$6.049*10^5$	54.62	0.0001
A	$7.819*10^5$	1	$7.819*10^5$	70.61	0.0001
B	$3.515*10^5$	1	$3.515*10^5$	31.75	0.0002
C	$8.106*10^5$	1	$8.106*10^5$	73.20	0.0001
E	$9.023*10^5$	1	$9.023*10^5$	81.49	0.0001
AB	$1.779*10^5$	1	$1.779*10^5$	16.07	0.0025

$$\varepsilon_{300}(\mu\varepsilon) = 1260.18 - 0.2474 * A - 0.0802 * B + 11.254 * C - 2.375 * E - 1.235 * 10^{-3} * A * B \quad (R^2 = 96.5) \tag{5}$$

Figures 9 to 12 show pavement responses for three shoulder geometry and material conditions. Weak short shoulder has a 100 mm width and 300 mm thickness and 30 MPa stiffness. Medium shoulder has a 913 mm width, 300 mm thickness and stiffness value of 450 MPa. Relatively strong shoulder has a 913 mm width, 500 mm thickness and 450 MPa stiffness. Figure 9 shows that for the same axle load and tire pressure, the deflection under the outer wheel load for the weak shoulder is more than double of the relatively strong shoulder and about 1.5 times the medium shoulder. This clearly emphasizes the importance of the shoulder stiffness represented by its width, thickness, and resilient modulus on the pavement response.

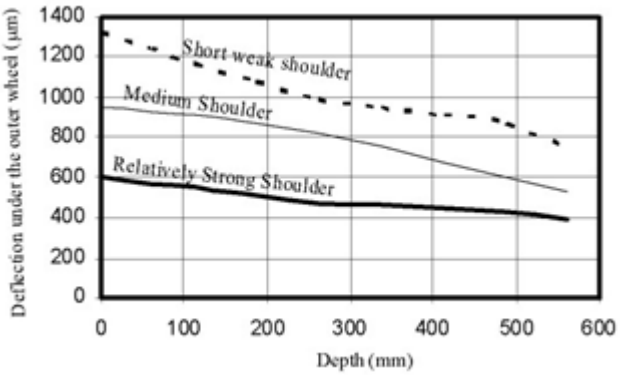

Figure 9. Comparison between the outer deflections for different shoulder conditions

Figures 10, 11 and 12 show that the weak short shoulder doesn't provide a good distribution of the load around the pavement edge and this causes the deflections, vertical compressive strains and compressive stresses to peak around the outer wheel on the top of the subgrade. This high concentration of deflections, stresses, and strains will lead to the edge failure. In the meanwhile, relatively strong shoulder provides a good spread of the loads, therefore, reducing deflections, stresses and strains on the top of the subgrade.

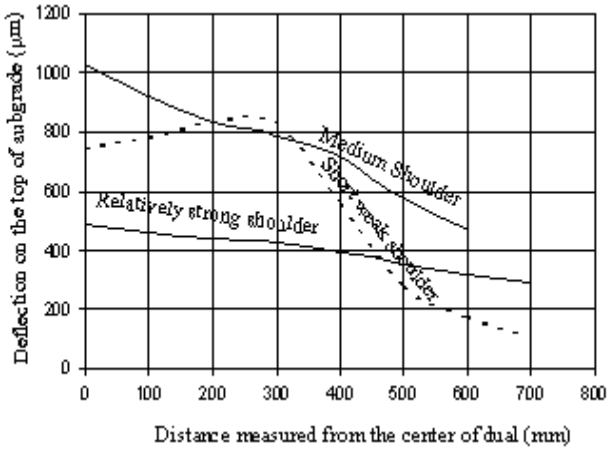

Figure 10. Comparison between deflections on the top of the subgrade for different shoulder conditions

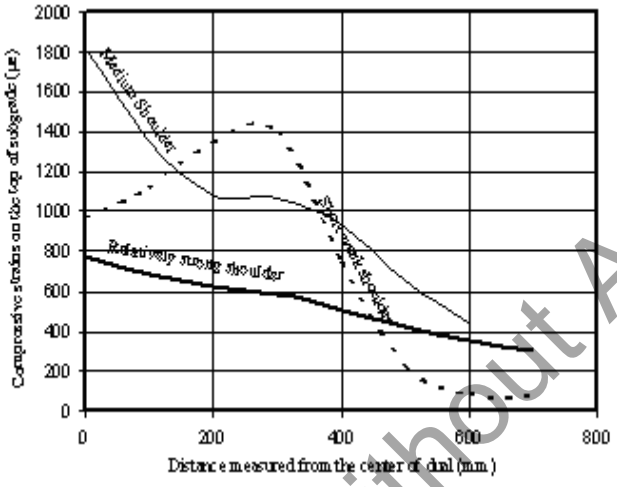

Figure 11. Comparison between the outer compressive strains on the top of the subgrade for different shoulder conditions

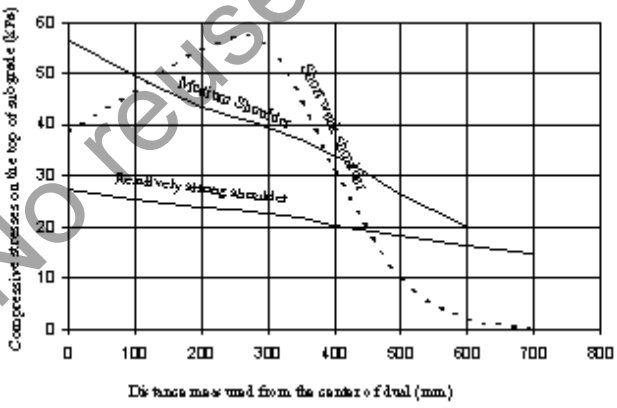

Figure 12. Comparison between the outer compressive stresses on the top of the subgrade for different shoulder conditions

7. Conclusions

From the factorial design, it is obvious that tire pressure is insignificant factor regarding the edge failure of pavements. Shoulder rigidity (i.e. stiffness) which is a function of the width, thickness and resilient modulus of the shoulder material, is a significant factor affecting the lateral support and therefore pavement response. Axle load is significant factor affecting the edge damage of the pavement. Using stiff shoulder will help reducing the concentration of deflections, stresses, strains on the top of the subgrade and will likely reduce the edge damage of the pavement. The order of importance of factors differs based on the pavement response under consideration.

Acknowledgements

The author would like to thank Opus International Consultants and the Foundation for Research, Science & Technology for funding which makes this research possible.

The author also would like to express his great gratitude to the Department of Civil Engineering, University of Canterbury, for its support.

References

Ball G.F. and Patrick, J. E., 2005, "A Study of Seal Edge Break Using RAMM Databases," Central Laboratories Report: 05-521068.00

Chandrupatla and Belegundu, 1996, "Introduction to Finite Elements in Engineering," Prentice-Hall, ISBN 0-13-061591-9.

Design Expert version 6, State-Ease Inc.2021 East Hennpin Ave., Suite 480, Minneapolis, MN 55413

Douglas C. M., 2001, "Design and Analysis of Experiments," John Wiley & Sons, Inc, 2001

Everstress version 5 for Windows software, Layered Elastic Analysis, Washington State Department of Transportation, March, 1999.

HIBBIT, KARLSSON and SORENSEN, INC., Getting Started with ABAQUS Standard, 2003.

Pidwerbesky, B. D., 1995, "Accelerated Dynamic Loading of Flexible Pavements at the Canterbury Accelerated Pavement Testing Indoor Facility," In Transportation Research Record 1482, TRB, National Research Council, Washington, D.C., pp. 79-86.

Wardle, L. J. Program CIRCLY, User's Manual, Geomechanics Computer program Number 2, Division of Applied Geomechanics, Commonwealth Scientific and Industrial Research Organisation, Melbourne, Australia, 1977.